PHYSICAL REVIEW B VOLUME 27, NUMBER 6 15 MARCH 1983

Electronic excitations in semiconductors with doping superlattices

P. Ruden and G. H. Döhler
Max-Planck-Institut für Festkörperforschung, Heisenbergstrasse 1, D-7000 Stuttgart 80, Federal Republic of Germany
(Received 20 September 1982)

Electron-hole excitation energies in the subband structure of semiconductors with doping superlattices are obtained from a discussion of the Bethe-Salpeter equation in a local representation. For two examples representing different subband structures due to different design parameters of the superlattice we present numerical results for intersubband excitations (spin-flip and non-spin-flip) with the wave vector along the superlattice axis. We include in the interaction term of the Bethe-Salpeter equation the electron-hole attraction and its associated exchange counterpart which corresponds to the resonant screening.

I. INTRODUCTION

A great deal of information about the interesting electronic structure of the dynamically two-dimensional charge carriers at interfaces and in semiconductor superlattices[1] can be obtained by the investigation of electronic excitations within the subband structure of these systems. Experimentally, these excitations are observable, e.g., in resonant Raman scattering[2–4] or in infrared-absorption experiments.[5,6] The observed resonances in the scattering cross section or the absorption coefficient do not, however, correspond immediately to single-particle transitions within the subband structure of the charge carriers. Many-body effects may appreciably influence the observed spectra. The importance of these many-body effects in Si metal-oxide-semiconductor (MOS) systems has been demonstrated in experimental and theoretical studies quite some time ago.[7–9] Recently, a new class of semiconductor superlattices became available with the successful growth of GaAs-doping superlattices or *n-i-p-i* crystals.

In a previous publication[10] (to be referred to as RDI) we have given a detailed description of the electronic band structure of semiconductors with doping superlattices. GaAs or, in one case, $Al_xGa_{1-x}As$ were considered as host materials. Examples were given how, through a judicious choice of design parameters (thickness of the doped layers and their doping concentration), an electronic subband structure may be tailored within wide limits. It was also indicated that owing to the feasibility of changing the charge-carrier concentration in a given *n-i-p-i* crystal (a unique feature of doping superlattices), many-body effects may conveniently be studied in these systems.

The self-consistent subband-structure calculations of RDI include self-energy corrections to the subband energies to the extent possible in the framework of the local-density-functional formalism.[11,12] In this paper we shall investigate electron-hole excitations within the electronic subband structure of a *n-i-p-i* crystal. For this purpose the Bethe-Salpeter equation for an electron-hole propagator is discussed in a local representation in Sec. II. Here we extend the work of previous authors on MOS systems[13] and $GaAs/Al_xGa_{1-x}As$ heterojunction superlattices[14] through the inclusion of a screened electron-hole attraction and by generalizing to the case of an arbitrary number of occupied subbands. In Sec. III we will present results of numerical calculations yielding electronic and coupled electron-phonon excitations with a nonzero wave vector in the direction of the superlattice axis (z).

II. BETHE-SALPETER EQUATION IN LOCAL REPRESENTATION

Quite generally we have for the (time-ordered) inverse dielectric function[15]

$$\kappa_t^{-1}(\vec{r}_1,t_1;\vec{r}_2,t_2)=\delta(\vec{r}_1-\vec{r}_2)\delta(t_1-t_2)+\int dt_3\int d^3r_3 v(\vec{r}_1-\vec{r}_3)\delta(t_1-t_3)\chi_t(\vec{r}_3,t_3;\vec{r}_2,t_2)\,, \tag{1}$$

where $v(\vec{r}_1-\vec{r}_2)$ is the Coulomb interaction. The density-density correlation function $\chi_t(\vec{r}_1,t_1;\vec{r}_2,t_2)$ is related to the electron-hole propagator through[16]

$$\chi_t(\vec{r}_1,t_1;\vec{r}_2,t_2)=\sum_{\xi_1,\xi_2} S(\{\vec{r}_1,t_1,\xi_1\},\{\vec{r}_1,t_1,\xi_1\};\{\vec{r}_2,t_2,\xi_2\},\{\vec{r}_2,t_2,\xi_2\}) . \tag{2}$$

In the following we will write for the sets of coordinates $\vec{r}_\lambda,t_\lambda,\xi_\lambda$ (position, time, spin) only the index λ. The Green's function $S(1,1';2,2')$ satisfies the Bethe-Salpeter equation

$$S(1,1';2,2')=S^0(1,1';2,2')+S^0(1,1';3,3')I(3,3';4,4')S(4,4';2,2') , \tag{3}$$

where integration or summation over repeated indices is implied. The noninteracting electron-hole propagator is given by

$$S^0(1,1';2,2')=g(1',2')g(2,1) , \tag{4}$$

where the single-particle Green's function $g(1,2)$ includes self-energy corrections. We now approximate the irreducible interaction $I(3,3';4,4')$ by (Fig. 1)

$$I(3,3';4,4')=\delta(3,3')\delta(4,4')v(3,4)-\delta(3,4)\delta(3',4')v^x(3,3') . \tag{5}$$

Here $v(3,4)$ is the Coulomb interaction and $v^x(3,3')$ is a screened Coulomb interaction.[17]

We shall include explicitly in our discussion of the response function only the (relatively few) additional charge carriers in subbands which are introduced into our system by doping and/or excitation. Therefore, we have to allow for the screening of the Coulomb interaction by the valence electrons of the host material. This can be done simply by dividing the Coulomb interaction by the dielectric constant of the host material, due to the fact that the subband wave functions are extended over macroscopic distances. However, since in the frequency range of interest this dielectric constant varies strongly, we shall also consider its frequency dependence (see below). In the part of $I(3,3';4,4')$ which describes the electron-hole attraction, however, the screening of the charge carriers in the subbands is to be included also.

We shall make a further approximation to the electron-hole attraction, which is in the spirit of the local-density-functional formalism.[17,18,9] It consists of replacing the dynamically screened Coulomb interaction $v^x(3,3')$ by a local static interaction given by

$$v^x(\vec{r}_3,\vec{r}_{3'})\simeq\frac{\delta v_{xc}(n(\vec{r}_3))}{\delta n}\delta(\vec{r}_3-\vec{r}_{3'}) , \tag{6}$$

where $v_{xc}(n)$ is the exchange and correlation contribution to the self-consistent potential as discussed in RDI.

If we now Fourier transform in time and space parallel to the layers, taking advantage of the translational invariance of the system parallel to the layers, we get from (2)–(6),

$$\chi(\vec{q}_{||},z_1,z_2,\omega)=\chi^0(\vec{q}_{||},z_1,z_2,\omega)+\int dz_3\int dz_4\chi^0(\vec{q}_{||},z_1,z_3,\omega)J(\vec{q}_{||},z_3,z_4)\chi(\vec{q}_{||},z_4,z_2,\omega) , \tag{7}$$

with

$$J(\vec{q}_{||},z,z')=v(\vec{q}_{||},z,z')+\frac{\partial v_{xc}(n(z))}{\partial n}\delta(z-z') \tag{8}$$

and

$$v(\vec{q}_{||},z,z')=\frac{2\pi e^2}{A\kappa_0}\frac{1}{q_{||}}e^{-q_{||}|z-z'|} . \tag{9}$$

By omitting the subscript t we indicate that we have gone over to the retarded density-density response function. As discussed in RDI we write the wave function of an electron in subband μ with wave vector $\vec{k}$ as

$$\psi_{\mu\vec{k}}(\vec{r})=\frac{1}{\sqrt{A}}e^{i\vec{k}_{||}\cdot\vec{r}_{||}}\xi_{\mu k_z}(z) . \tag{10}$$

In what follows, the small dispersion along k_z of the electrons will be neglected and their energy and wave function can be written as

$$\epsilon_{\mu\,\vec{k}}=\epsilon_{\mu\,\vec{k}_{||}}=\epsilon_{\mu}+\frac{\hbar^2 k_{||}^2}{2m^e}\ , \tag{11}$$

$$\psi_{\mu\,\vec{k}}(\vec{r})=\frac{1}{\sqrt{A}}e^{i\vec{k}_{||}\cdot\vec{r}_{||}}\frac{1}{\sqrt{N_{\rm SL}}}\sum_m e^{ik_z md}\Phi_\mu(z-md)\ , \tag{12}$$

where the functions $\Phi_\mu(z-md)$ are strongly localized in the n-type layer of index m and do not overlap with those localized in neighboring layers, and $N_{\rm SL}$ is the number of superlattice periods.

At $T=0$ K, $\chi^0(\vec{q}_{||},z_1,z_2,\omega)$ is, therefore, given by

$$\chi^0(\vec{q}_{||},z_1,z_2,\omega)=2\sum_{\vec{k}_{||}}\sum_{k_z,k_z'}\frac{\rho(\epsilon_{\mu\,\vec{k}_{||}})-f(\epsilon_{\mu,\,\vec{k}_{||}+\vec{q}_{||}})}{\epsilon_{\mu\,\vec{k}_{||}}-\epsilon_{\mu,\,\vec{k}_{||}+\vec{q}_{||}}-\hbar\omega-i\delta}\xi^+_{\mu' k_z'}(z_1)\xi_{\mu k_z}(z_1)\xi^+_{\mu k_z}(z_2)\xi_{\mu' k_z'}(z_2)\ . \tag{13}$$

Owing to the periodicity property of the superstructure we can transform the integral equation (7) into a matrix equation

$$\chi_{GG'}(\vec{q}_{||},q_z,\omega)=\chi^0_{GG'}(\vec{q}_{||},\omega)+\sum_{G_1,G_2}\chi^0_{GG_1}(\vec{q}_{||},\omega)J_{G_1G_2}(\vec{q}_{||},q_z)\chi_{G_2G'}(\vec{q}_{||},q_z,\omega)\ . \tag{14}$$

Here $J_{GG'}(\vec{q}_{||},q_z)$ is the Fourier transform of $J(\vec{q}_{||},z,z')$ defined in Eq. (8) and G,G' are reciprocal-superlattice vectors. Since we have taken the dispersion as strictly two dimensional, $\chi^0(\vec{q}_{||},\omega)$ does not depend on q_z. The response function $\chi(\vec{q}_{||},z,z',\omega)$ will be of a similar separable form as $\chi^0(\vec{q}_{||},z,z',\omega)$. Thus using (12) we can transform Eq. (14) into a local representation[19,20]:

$$\begin{aligned}\sum_{\substack{\mu,\mu'\\ \nu,\nu'}}A_{\mu\mu'}(q_z+G)\chi_{\mu\mu'\nu\nu'}(\vec{q}_{||},q_z,\omega)A^\dagger_{\nu\nu'}(q_z+G')&=\sum_{\substack{\mu,\mu',\\ \nu,\nu'}}A_{\mu\mu'}(q_z+G)\chi^0_{\mu\mu'\nu\nu'}(\vec{q}_{||},\omega)A^\dagger_{\nu\nu'}(q_z+G')\\ &+\sum_{\substack{\mu,\mu',\\ \nu,\nu'}}\sum_{\substack{\sigma,\sigma',\\ \tau,\tau'}}A_{\mu\mu'}(q_z+G)\chi^0_{\mu\mu'\nu\nu'}(\vec{q}_{||},\omega)\\ &\times\left[\sum_{G_1G_2}A^\dagger_{\nu\nu'}(q_z+G_1)J_{G_1G_2}(\vec{q}_{||},q_z)A_{\sigma\sigma'}(q_z+G_2)\right]\\ &\times\chi_{\sigma\sigma'\tau\tau'}(\vec{q}_{||},q_z,\omega)A^\dagger_{\tau\tau'}(q_z+G')\end{aligned} \tag{15}$$

with

$$A_{\mu\mu'}(q_z+G)=\int dz\,\Phi^*_\mu(z)\Phi_{\mu'}(z)e^{i(q_z+G)z}\ . \tag{16}$$

We can write Eq. (15) as

$$A\chi A^\dagger=A\chi^0A^\dagger+A\chi^0A^\dagger JA\chi A^\dagger=A\chi^0(1+A^\dagger JA\chi^0+\cdots)A^\dagger=A\chi^0(1-A^\dagger JA\chi^0)^{-1}A^\dagger\ , \tag{17}$$

if, for the sake of clarity, we suppress all indices and variables.

From the last equation it is apparent that the poles of $\chi_{GG'}(\vec{q}_{||},q_z,\omega)$, which coincide with the collective excitations of the system, are given by the condition

$$\det(1-A^\dagger JA\chi^0)=0\ . \tag{18}$$

Equation (18) provides the elementary electronic excitations in the subband structure of the superlattice. With the self-consistently calculated subband wave functions and energies (as discussed in RDI) all the quantities needed in Eq. (18) can be calculated. The size of the matrices is determined by the number of

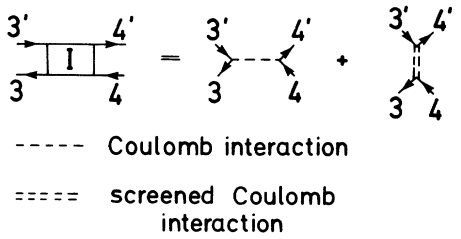

FIG. 1. Graphical representation of the interaction term in the Bethe-Salpeter equation. The numbers stand for sets of coordinates including position, time, and spin. For the numerical calculations the dynamically screened Coulomb interaction of the electron-hole attraction has been approximated by a local static interaction.

subbands populated and by the frequency range to be investigated. In our examples it was sufficient to use the six lowest subbands so that the largest matrices needed were 36×36 matrices.

Considering only a single subband, one obtains the plasmons of a dynamically two-dimensional multilayer system which were discussed (neglecting the electron-hole attraction) extensively by various authors.[21–24] An interesting feature of doping superlattices with respect to plasmon excitations is the fact that they represent ideal candidates for the observation of acoustic plasmons. These originate from the spatially separated dynamically two-dimensional electron and hole systems which under suitable conditions[10] exist in *n-i-p-i* crystals.

In this paper, however, we discuss only excitations within the subband system of the electrons. If electrons are present in the *n*-type layers *and* holes in the *p*-type layers, excitations in the subband system of the electrons generally couple via the Coulomb interaction to excitations within the *p*-type layers, even in the absence of an overlap of electron and hole wave functions. In the case of a vanishing wave-vector component parallel to the layers, however, these excitations are decoupled. Therefore, the existence of holes in the *p*-type layers can be ignored in this case.

III. RESULTS FOR COLLECTIVE INTERSUBBAND EXCITATIONS WITH $\vec{q}_{||}=0$

In this section we shall discuss results of Eq. (18) for $\vec{q}$ approaching zero along the z direction. The excitations given by (18) thus correspond to those observed in Raman scattering experiments in the backscattering geometry. Since the spin-orbit coupling in GaAs leads to valence-band states of mixed spin it is possible to observe Raman transitions which involve a flip of the electronic spin. These spin-flip transitions observe different polarization selection rules than the non-spin-flip transitions.[25,26] We shall consider the former first.

A. Spin-flip excitations

As is obvious from the diagrams of Fig. 1, the first term in (5) which corresponds to the resonant screening vanishes if electron and hole do not have the same spin. Thus only the electron-hole attraction is to be included in the irreducible interaction of the Bethe-Salpeter equation. Making the same approximations as above and neglecting that the electron-hole interaction described by (6) should be different for the spin-flip case, we find that spin-flip excitations are found from

$$\det(1-A^{\dagger}\tilde{J}A\chi^{0})=0\,, \tag{19}$$

where $\tilde{J}$ includes only the second term in Eq. (8).

For the lowest excitations as a function of the variable carrier concentration in a *n-i-p-i* multilayer structure with the design parameters $d_n=d_p=40$ nm, $d_i=0$, and $n_D=n_A=10^{18}$ cm^{-3} (this corresponds to the first example in RDI, we use the same notation), we find the results shown in Fig. 2. The solid lines, which give the result of Eq. (19), lie everywhere below the subband separations (dashed-dotted lines) as they should due to the attractive nature of the electron-hole interaction. It can also be seen from Fig. 2 that the excitation energy corresponding to the $(\mu=0)\rightarrow(\mu'=1)$ transition coincides over a wide range with the subband separation in the Hartree approximation (dotted lines). Since (as was discussed in RDI) the envelope functions $\Phi_{\mu}(z)$ are , for the lowest μ, in this system very nearly harmonic-oscillator functions, the shift of the Hartree subband separation due to the exchange and correlation correction can be calculated analytically to lowest order in the carrier concentration. The shift due to the electron-hole interaction can also be calculated analytically in lowest order for harmonic-oscillator functions and is found to be equal in magnitude and opposite in sign to the ex-

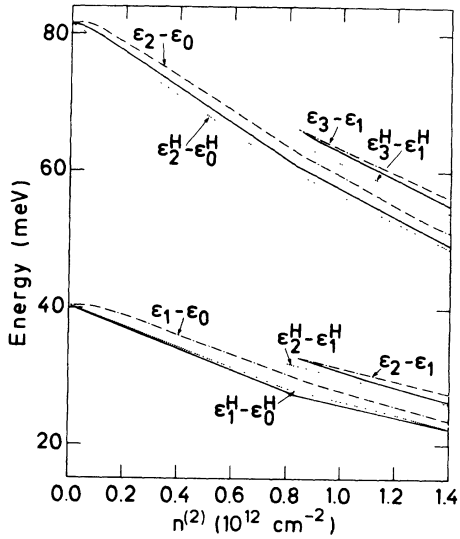

FIG. 2. Lowest spin-flip excitations for $\vec{q}_{||}=0$ in an *n-p* multilayer crystal with doping parameters $n_D=n_A=10^{18}$ cm^{-3}, $d_n=d_p=40$ nm, and $d_i=0$ as a function of the two-dimensional carrier concentration. The dashed-dotted and dotted lines represent the separations of occupied nearest-neighbor and next-nearest-neighbor subbands in the local-density-functional and Hartree approximation, respectively. The solid lines show the corresponding spin-flip excitations with the electron-hole attraction taken into account.

change and correlation correction.[27] This cancellation should not be overrated as it applies only to the lowest transition in this special system.

For the *n-i-p-i* superlattice discussed as the second example in RDI (design parameters $d_n = d_p = 4$ nm, $d_i = 36$ nm, and $n_D = n_A = 5.25 \times 10^{18}$ cm^{-3}) we find the spin-flip excitation energies shown in Fig. 3. Here the electron-hole attraction does not quite cancel the shift due to exchange and correlation in the $(\mu = 0) \rightarrow (\mu' = 1)$ transition.

B. Non-spin-flip excitations

To find these excitation energies we have to look for solutions of Eq. (18). We first take the screening of the host lattice in the Coulomb interaction as static. In this approximation we find for the *n-p* multilayer structure described above the excitation energies shown in Fig. 4. The solid lines which correspond to the excitation energies intersect the dashed-dotted lines representing the subband separation at low carrier concentration. This means that at low carrier concentration the electron-hole attraction dominates its exchange counterpart which in turn becomes very important at higher carrier densities. The dotted line shows the excitation energies with the electron-hole interaction neglected. Peculiar in this system is that the resonant screening compensates almost exactly the diminishing subband separation for the $(\mu = 0) \rightarrow (\mu' = 1)$ transition. This result is also corroborated by an analytic calculation to lowest order.[27] For the *n-i-p-i* superlattice with wide intrinsic layers we find the results shown in Fig. 5.

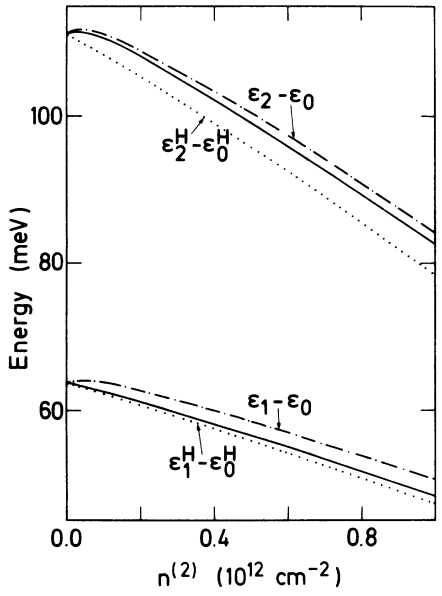

FIG. 3. Lowest spin-flip excitations for $\vec{q}_{||} = 0$ in an *n-i-p-i* crystal with the design parameters $n_D = n_A = 5.25 \times 10^{18}$ cm^{-3}, $d_n = d_p = 4$ nm, and $d_i = 36$ nm as a function of the two-dimensional carrier concentration. The dashed-dotted lines represent the separations of occupied nearest-neighbor and next-nearest-neighbor subbands in the local-density-functional and Hartree approximation, respectively. The solid lines show the corresponding spin-flip excitations with the electron-hole attraction taken into account.

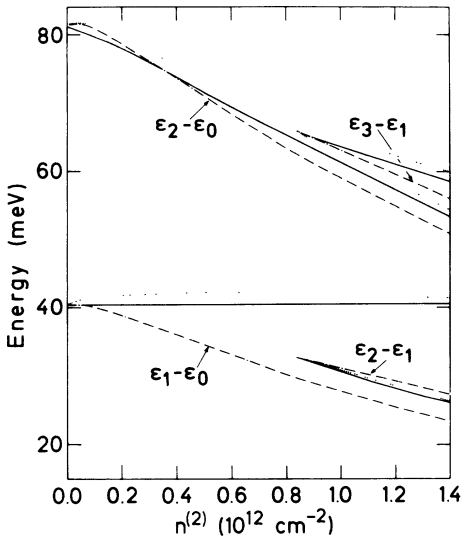

FIG. 4. Lowest non-spin-flip excitations in an *n-p* multilayer crystal with doping parameters $n_D = n_A = 10^{18}$ cm^{-3}, $d_n = d_p = 40$ nm, and $d_i = 0$ as a function of the two-dimensional carrier concentration. The dashed-dotted lines represent the separations of occupied nearest-neighbor and next-nearest-neighbor subbands. The solid lines show the excitation energies with the electron-hole attraction and the resonant screening taken into account. The dotted lines show excitation energies with the electron-hole interaction neglected.

The excitation energies lie close to the LO-phonon frequency of the host material for our particular *n-p* multilayer structure. In this range the dielectric constant of the lattice varies rapidly with frequency and this should be taken into account in the Coulomb interaction. As briefly mentioned above, we shall do this by replacing the static dielectric constant of the host material κ_0 in Eq. (9) by

$$\kappa(\omega) = \kappa_0 \frac{\omega_T^2}{\omega_L^2} \frac{\omega_L^2 - \omega^2}{\omega_T^2 - \omega^2} . \tag{20}$$

It would, however, be incorrect to screen the electron-hole attraction dynamically simply by using (20) as can be seen from the diagrams of Fig. 1.

On the other hand, as we have seen in Fig. 2, the electron-hole attraction largely cancels the shift in the subband separation originating from the ex-

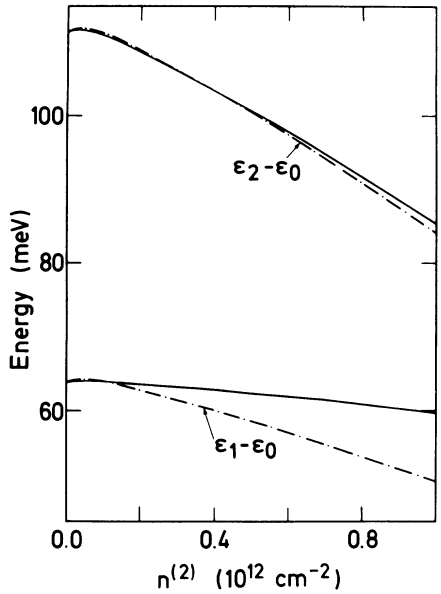

FIG. 5. Lowest non-spin-flip excitations in an *n-i-p-i* crystal with the design parameters $n_D=n_A=5.25\times10^{18}$ cm^{-3}, $d_n=d_p=4$ nm, and $d_i=36$ nm as a function of the two-dimensional carrier concentration. The dashed-dotted lines represent the separation of occupied nearest-neighbor and next-nearest-neighbor subbands. The solid lines show the excitation energies with resonant screening and electron-hole interaction taken into account.

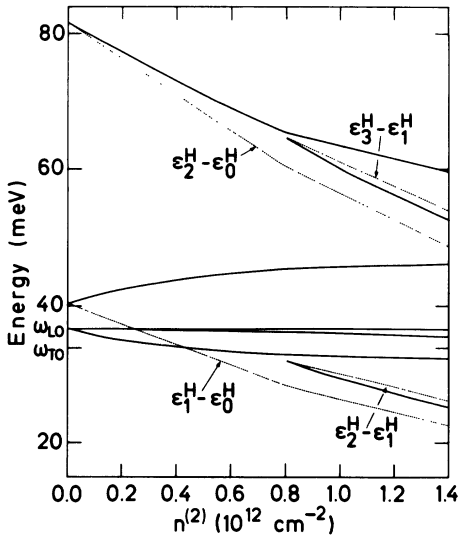

FIG. 6. Lowest non-spin-flip coupled electron-phonon excitations for an *n-p* multilayer crystal with the doping parameters $n_D=n_A=10^{18}$ cm^{-3}, $d_n=d_p=40$ nm, and $d_i=0$ as a function of the two-dimensional carrier concentration. The dotted lines represent the separations of occupied nearest-neighbor and next-nearest-neighbor subbands in the Hartree approximation. The solid lines show the excitation energies with the electron-hole interaction neglected and the Coulomb interaction in the first term of Eq. (8) dynamically screened by the host lattice. For clarity we have not shown several modes which originate from the relatively weak coupling of higher electronic modes with the LO phonon and which, therefore, lie very close beneath the LO-phonon frequency.

change and correlation potential. We shall, therefore, neglect the exchange and correlation shift in the subband separation along with the electron-hole attraction in the calculation of coupled electron-phonon excitations in order to avoid the problem of calculating the dynamically screened electron-hole attraction. The results of this procedure are shown in Fig. 6 for the *n-p* multilayer structure cited above. The solid lines represent the coupled electron—LO-phonon excitations and the dotted lines represent the subband separations in the Hartree approximation. In the case of the *n-i-p-i* crystal with wide intrinsic layers (second example) the excitation energies are relatively far above the phonon frequencies and their coupling is therefore weak.

IV. CONCLUSIONS

Doping superlattices represent an interesting system for the experimental and theoretical study of many-body effects. To show this we have calculated electronic and coupled electron-phonon excitations for two different *n-i-p-i* crystals as a function of the charge-carrier concentration.

For the case of the vanishing wave vector parallel to the layers we have obtained numerical results for the intersubband excitations in doping superlattices with several subbands occupied. In the case of spin-flip excitations (or spin-density excitations) we find a reduction of the excitation energies below the values of the corresponding subband separations due to electron-hole attraction. In doping superlattices with sufficiently wide regions of homogeneous *n*-type doping the electron-hole attraction compensates the exchange-correlation corrections to the energies of the lowest and first excited subbands in the limit of low subband populations within our local-density approximation. In the case of non-spin-flip excitations (charge-density excitations), except for very low carrier concentrations, a net shift to higher energies is observed because of the resonant screening.

For doping superlattices with a sufficiently wide region of homogeneous *n*-type doping we have found that this shift compensates the decrease of subband separation between the lowest and the first excited subband as a function of increasing subband population for low concentrations exactly and at high concentration at least rather exactly (except for variation due to the frequency dependence of the

dielectric susceptibility of the host material). Thus the non-spin-flip excitations between the lowest and the first excited subband of such a system occur almost exactly at the bulk-plasmon frequency $\omega_p(n_D)$ of a homogeneous bulk semiconductor of the same doping concentration. They are nearly independent of the population of the subbands, provided that $\omega_p(n_D)$ is sufficiently different from the LO-phonon frequency ω_L.

We have not taken into account any broadening effects due to the finite lifetime of the excitations in our calculations since it is difficult to go beyond a phenomenological treatment of this problem. We realize, however, that these effects may appreciably influence the shape of observed spectra.[7] There is no essential difficulty involved in treating excitations with nonvanishing wave-vector components parallel to the layers if there are no holes in the p-type layers of a doping superlattice. In this case plasmonlike excitations originating from electronic intrasubband transitions appear and also coupled plasmon-intersubband excitations. The case of excitations with finite wave-vector components parallel to the layers in a n-i-p-i crystal with layers of electrons *and* holes, however, requires the inclusion of the polarizabilities of both types of charge carriers since the Coulomb interaction couples the electronic excitations within the n-type to those of the holes in the p-type layers. We shall further investigate this interesting situation.

ACKNOWLEDGMENT

We would like to thank W. Hanke for stimulating discussions.

[1]T. Ando, A. Fowler, and F. Stern, Rev. Mod. Phys. 54, 437 (1982), and references therein.

[2]E. Burstein, A. Pinzuk, and S. Buchner, in *Proceedings of the 14th International Conference on the Physics of Semiconductors,* edited B. L. H. Wilson (IOP, Bristol, 1978), Vol. 43, p. 1231.

[3]G. Abstreiter and K. Ploog, Phys. Rev. Lett. 42, 1308 (1979).

[4]A. Pinczuk, H. L. Störmer, R. Dingle, J. M. Worlock, W. Wiegmann, and A. C. Gossard, Solid State Commun. 32, 1001 (1979).

[5]J. F. Koch, Surf. Sci. 58, 104 (1976).

[6]J. P. Kotthaus, in *Proceedings of the 15th International Conference on the Physics of Semiconductors, Kyoto, Japan, 1980* [J. Phys. Soc. Jpn. 49, Suppl. A, 937 (1980)].

[7]S. J. Allen, D. C. Tsui, and B. Vinter, Solid State Commun. 20, 425 (1976).

[8]B. Vinter, Phys. Rev. B 15, 3947 (1977).

[9]T. Ando, Z. Phys. B 26, 263 (1977).

[10]P. Ruden and G. H. Döhler, preceding paper, Phys. Rev. B 27, 3538 (1983).

[11]P. Hohenberg and W. Kohn, Phys. Rev. 136, B864 (1964).

[12]W. Kohn and L. J. Sham, Phys. Rev. 140, A1133 (1965).

[13]D. A. Dahl and L. J. Sham, Phys. Rev. B 16, 651 (1977).

[14]T. Ando and S. Mori, J. Phys. Soc. Jpn. 47, 1518 (1979).

[15]L. Hedin and S. Lundquist, in *Solid State Physics,* edited by H. Ehrenreich, F. Seitz, and D. Turnbull (Academic, New York, 1969), Vol. 23.

[16]A. F. Fetter and J. D. Walecka, *Quantum Theory of Many-Particle Systems* (McGraw-Hill, New York, 1971).

[17]W. Hanke and L. J. Sham, Phys. Rev. B 21, 4656 (1980).

[18]S. K. Sinha, in *Dynamical Properties of Solids,* edited by G. K. Horton and A. A. Maradudin (North-Holland, Amsterdam, 1979), Vol. 3.

[19]W. Hanke, Adv. Phys. 27, 287 (1978).

[20]L. J. Sham, in *Dynamical Properties of Solids,* edited by G. K. Horton and A. A. Maradudin (North-Holland, Amsterdam, 1974), Vol. 1.

[21]A. L. Fetter, Ann. Phys. (N.Y.) 88, 1 (1974).

[22]D. Green, Phys. Rev. B 8, 1958 (1973).

[23]M. Apostol, Z. Phys. B 22, 13 (1975).

[24]S. Das Sarma and J. J. Quinn, Phys. Rev. B 25, 7603 (1982).

[25]See for example, M. Klein, in *Light Scattering in Solids,* edited by M. Cardona (Springer, Berlin, 1975).

[26]E. Burstein, A. Pinczuk, and D. L. Mills, Surf. Sci. 98, 451 (1980).

[27]P. Ruden, Ph.D. thesis, University of Stuttgart, 1982 (unpublished).